

Development of a single-mode DFB heterolaser with inclined radiation output

© V.R. Baryshev¹, E.D. Egorova¹, N.S. Ginzburg¹, E.R. Kocharovskaya¹, A.M. Malkin¹, V.Yu. Zaslavsky¹, C.B. Morozov², A.S. Sergeev¹

¹ Institute of Applied Physics, Russian Academy of Sciences, 603155 Nizhny Novgorod, Russia

² Institute of Physics of Microstructures, Russian Academy of Sciences, 603950 Nizhny Novgorod, Russia

E-mail: baryshev@appl.sci-nnov.ru

Received May 5, 2023

Revised June 29, 2023

Accepted July 6, 2023

We study a possibility of implementing a single-mode DFB heterolaser with inclined (with respect to the surface of the structure) output of the generated radiation. We find the periodic dielectric structure shape that makes it possible to realize the distributed feedback for wavebeams propagating along the structure and, at the same time, to ensure the output of up to 70% of the generated radiation power in the inclined direction. Within the framework of the semiclassical quasi-optical model, the possibility of stationary lasing regimes is shown for finite lateral dimensions of the Bragg structure.

Keywords: heterolaser, Bragg structures, distributed feedback, radiation output.

DOI: 10.61011/SC.2023.05.57153.41k

1. Introduction

The generation of spatially coherent high-power radiation remains one of the important problems in the physics of semiconductor laser structures. Expanding the active volume is a natural way to increase the power of lasing. To establish the single-mode lasing, Bragg resonators [1,2] made in the form of dielectric structures with a periodically varying refraction index, which allow providing the distributed feedback (DFB), have been widely used. In the case of lasers based on semiconductor heterostructures, Bragg gratings can be applied on the surface using various lithography methods, and can also be incorporated inside the structure.

One of the problems in ensuring mode selection in lasers with an active medium, which is characterized by high gain per pass, is reflection from the edges of the waveguide, which can create a parasitic feedback loop that increases the Q-factor of many modes and potentially makes it difficult to establish the single-mode lasing. To suppress these negative effects, this study proposes to use a Bragg structure, which simultaneously provides the necessary feedback and at the same time scatters the main part of the generated radiation into coherent beams propagating at an angle to the surface of the structure [3–8]. This scattering occurs over the entire area of the active region, which potentially makes it possible to minimize the effect of reflections from the ends of the waveguide layer. Moreover, in a laser with radiation output at an angle to the surface of the structure, the region of population inversion can be effectively limited to a zone inside the grating, which can be separated from the edges by absorption regions in the non-inverted zone of

the heterostructure, which also reduces the effect of edge reflections.

This study considers a flat dielectric multilayer structure with a Bragg grating applied on its surface (Figure 1). The structure consists of a substrate, a waveguide layer with a high refraction index, and an active layer, which is thin enough not to significantly change the spectrum of eigenmodes. The prototype of this structure is the planar cadmium-mercury-tellurium (CMT) nanoheterostructure with a lasing wavelength of $3.75\ \mu\text{m}$ [9–11]. A rectangular Bragg grating can be applied using lithography methods on the surface of the waveguide layer.

2. Radiation output at an angle to the surface of the waveguide structure

First, let us consider the problem of scattering of a dielectric waveguide mode (which, in principle, can have TE or TM polarization) on a corrugated surface section, made in the form of modulation of the dielectric constant of the medium in the form of a meander with a depth of b_{gr} with the dielectric constant (Figure 1):

$$\varepsilon = 1 + \frac{(\varepsilon_b - 1)}{2} (1 + \text{sgn}(\sin(\bar{h}z))), \quad (1)$$

where sgn is a function equal to 1 for positive values of the argument and -1 for negative ones, $\bar{h} = 2\pi/d$, d is corrugation period, ε_b is dielectric constant of the corrugation material. In a regular waveguide, an eigenmode with fields $\sim e^{i\omega t - ihz}$ is characterized by the known dispersion characteristic $h(\omega)$ [1], which relates the longitudinal wave number h with frequency ω . In this case, the ratio

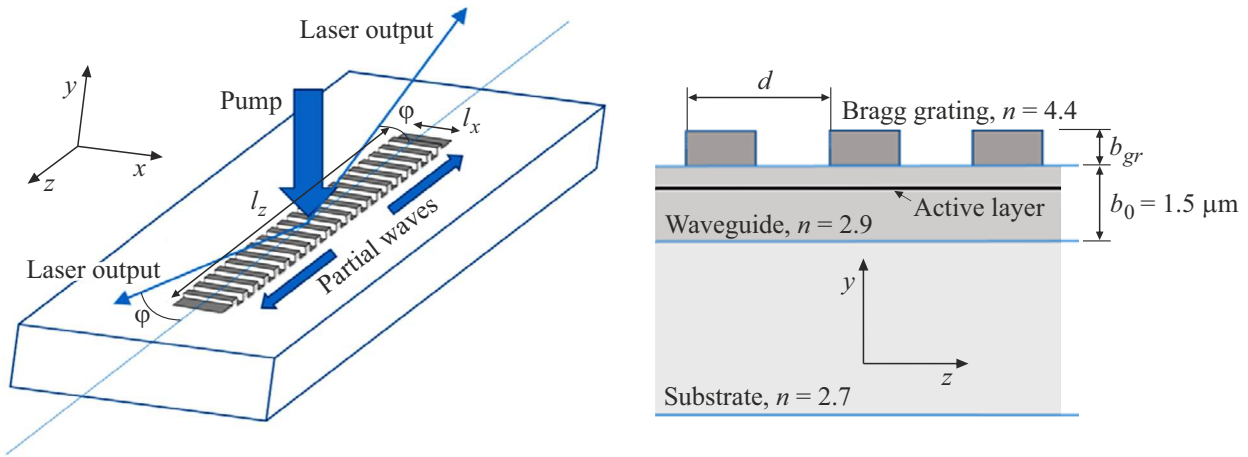


Figure 1. Diagram of a DFB laser with transverse radiation output based on CMT heterostructures.

$n_{\text{eff}} = hc/\omega$, where c is speed of light in vacuum, will be called the effective refractive index of the waveguide layer. The corrugated section (1) can be considered as a diffraction grating that scatters the wave in directions determined by the conditions of synchronism with the corresponding harmonics of the corrugation. Thus, the vector potential of the scattered field in free space above the waveguide can be represented as the sum

$$\mathbf{A} = \mathbf{x}_0 \text{Re} \left(\sum_{s=-\infty}^{\infty} C_s e^{i\omega t - ih_s z - ig_s x} \right), \quad (2)$$

where $h_s = h + s\bar{h}$ and g_s are longitudinal and transverse wave numbers of scattered waves (beams), related by the dispersion relation

$$(h + s\bar{h})^2 + g_s^2 = \frac{\omega^2}{c^2}. \quad (3)$$

It follows from (3), that propagating, and therefore carrying away the energy of the waveguide mode, are only waves for which

$$\frac{\omega^2}{c^2} - (h + s\bar{h})^2 > 0.$$

It should be separately noted here that for a symmetric structure, series (2) will contain only terms with odd subscripts. A special role is played by the case of Bragg resonance, when for a certain selected subscript $s = S$ the following condition is satisfied:

$$2h \approx S\bar{h}, \quad (4)$$

with which the scattering occurs in the dielectric waveguide mode propagating in the direction opposite to the original one. Thus, with condition (4) fulfilled, structure (1), in addition to scattering into waves propagating at an angle to the surface, provides coupling and mutual scattering of two counterpropagating wave flows, which can be characterized

by the vector potential \mathbf{A} and represent in the following form

$$\mathbf{A} = \mathbf{x}_0 \text{Re} \left(a(y) (C_+(x, z, t) e^{-ihz} + C_-(x, z, t) e^{ihz}) e^{i\omega t} \right), \quad (5)$$

where $a(y)$ is a normalized function determined by the field structure of the corresponding n -mode of a regular dielectric waveguide, \mathbf{x}_0 is unit vector; $C_{\pm}(x, z, t)$ are complex amplitudes of partial waves. In this case, wave flows (5) excite runaway waves in other diffraction orders that meet condition (3).

The Bragg structure can be used as a resonator for a laser [1,2], provided that the Bragg frequency determined by (4) is within the gain band of the active medium. Then, for definiteness, it is assumed that the Bragg frequency with the central frequency of the amplification band is $\omega = \omega_0 = 2\pi c/\lambda_0$, λ is the central wavelength of the radiation. In this case, the choice of polarization is carried out by the active layer. In this study we investigate the case when only TE-polarized waves are amplified [10,12].

According to (3) and (4), scattered waves are propagating if

$$\begin{aligned} \frac{\omega^2}{c^2} - h_s^2 &= \frac{\omega^2}{c^2} - h^2 \left(1 \pm \frac{2s}{S} \right)^2 \\ &= h^2 \left(n_{\text{eff}}^{-2} - \left(1 \pm \frac{2s}{S} \right)^2 \right) > 0. \end{aligned} \quad (6)$$

When this inequality is satisfied, waves (5) are scattered in the $y - z$ plane, which results in energy emission from the waveguide at a certain angle of $\varphi_s = \text{arctg}(g_s/h_s)$ to the surface (Figure 1); otherwise, the spatial harmonic of the waves (2) is exponentially pressed against the grating and does not transfer energy. Accordingly, the number of possible radiation directions depends on the spatial index s and on the effective refractive index of the unperturbed dielectric waveguide at the central frequency of the gain band of the active medium $n_{\text{eff}} = h/\frac{\omega_0}{c} = h\lambda_0/2\pi$ and is

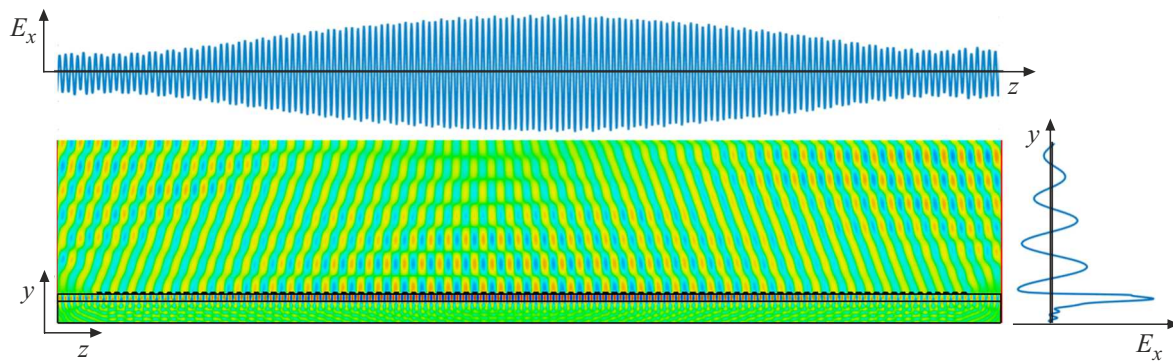


Figure 2. Longitudinal and transverse distributions of the E_x component of the electric field for the fundamental mode of the Bragg resonator.

determined by the number of integer solutions to the following inequality:

$$\frac{1 - n_{\text{eff}}^{-1}}{2} S < s < \frac{1 + n_{\text{eff}}^{-1}}{2} S, \quad (7)$$

where s being number of the harmonic of the scattering. The angle between the harmonic wave vector and the surface of the structure is determined by the following relationship:

$$\text{tg } \varphi_s = \sqrt{\left(\frac{S}{n_{\text{eff}}(S - 2s)}\right)^2 - 1}. \quad (8)$$

Due to the fact that each of the two partial waves C_{\pm} is scattered independently, additional beams appear in pairs in $\pm\varphi$ directions. At the same time, there is one important exception to the formation of the $\varphi = 90^\circ$ vertical beam: if S is even, then there is always one solution to (7) in the form of $s = S/2$ that provides both partial waves to be scattered perpendicular to the surface of the waveguide. Although the use of a vertical beam to output radiation in one direction normal to the grating surface seems preferable at first glance, this option is complicated by the interference between counterpropagating partial waves. As is known, the eigenmodes of a Bragg resonator are represented as a combination of two counterpropagating partial waves (5) with one field variation along the length of the resonator. In this case, there is a degeneracy in Q-factor for the modes with eigenfrequencies above and below the Bragg cutoff band (HF and LF) of the mode. As shown in [12], adding a vertical radiation channel is effective for the HF mode; in this case Q-factor of the above-mentioned mode decreases and, in the presence of an active medium, a LF mode will be excited, for which, due to the above-specified interference, the transverse output is ineffective. Thus, the vertical radiation channel provides mode selection, however, when a higher Q-factor LF mode is excited, the transverse radiation output is almost absent. It should be noted that in [13–15] an alternative method for selecting HF and LF modes was proposed, based on the finiteness of the transverse (lateral) size of the Bragg structure, where

it was shown that with the transverse dimensions of the above-specified structure l_x , meeting the Fresnel condition of $F = \sqrt{2\pi l_x}/l_x \sqrt{h} \leq 1$, the transverse diffraction losses of the LF mode are significantly less than for the HF mode.

Then in this study, the case of symmetric grating is considered, for which scattering with even harmonic indices s is prohibited. The Bragg resonance in the third order of diffraction (i.e., at $S = 3$) allows scattering into only one additional beam corresponding to $s = 1$.

3. Analysis of eigenmodes of a Bragg structure with radiation output at an angle to the surface

In this Section, eigenmodes of the Bragg structure are studied within the two-dimensional model using the CST Microwave Studio software package. The eigenmode with the highest Q-factor taking into account the distribution of energy losses over various radiation channels, can be found by solving a non-stationary problem based on excitation of the resonator by an external electromagnetic pulse (Figure 2). In the process of attenuation of the initial perturbations, the highest-Q mode should stand out. The modeling was carried out for the structure of the CMT laser mentioned in the Introduction with a wavelength of $\lambda_0 = 3.75 \mu\text{m}$, with a Bragg grating made of amorphous germanium. Parameters of the structure are listed in the table. Width of the initial pulse spectrum was limited by

Parameters of the structure

Thickness of the waveguide layer, b_0	1.5 μm
Refraction index of the waveguide layer	2.9
Substrate thickness	5 μm
Substrate dielectric constant	2.7
Corrugation depth, b_{gr}	0.4 μm
Refraction index of corrugation	4.4
Corrugated area length, l_z	(60–240 μm)
Corrugation period, d	1.98 μm
Laser wavelength, λ_0	3.75 μm

the value at which only the spectrum of low-frequency modes was excited, i.e. the modes with eigenfrequencies below the opacity zone. The longitudinal structure of the mode along the z axis inside the waveguide for a mode with a central frequency of 80 THz, corresponding to the λ_0 wavelength, is shown in Figure 2 (top graph) and represents the interference of two counterpropagating partial waves. The distribution of the electromagnetic field along the normal coordinate y (Figure 2, right) is close to the eigenmode of a conventional planar dielectric waveguide. In the structure of the field above the surface of the waveguide, two beams with flat phase fronts are distinguished (Figure 2, bottom). However, the modeling shows that similar beams also propagate down into the substrate. The power balance between the surface output and the loss channel into the structure depends on the depth of the Bragg grating. The optimal depth value of $b_{gr}^{opt} = 0.4 \mu\text{m}$ allows up to 70% of the emitted power to be directed upward at an angle of $\varphi \sim 20^\circ$ to the surface of the structure.

Then in Section 4, to analyze the nonlinear dynamics of the DFB laser, the coupled wave method will be used, within which it is assumed that counterpropagating wave flows are coupled on a Bragg grating, and harmonics emitted at an angle represent a loss channel additional to ohmic losses. In this approximation, the mutual scattering of partial waves (3) on structure (1) can be described within the coupled wave method [1,2]:

$$\begin{aligned} \frac{1}{v_{gr}} \frac{\partial C_+}{\partial t} + \frac{\partial C_+}{\partial z} + \gamma C_+ + i\alpha C_- &= 0, \\ \frac{1}{v_{gr}} \frac{\partial C_-}{\partial t} + \frac{\partial C_-}{\partial z} + \gamma C_- + i\alpha C_+ &= 0, \end{aligned} \quad (9)$$

where α is coupling coefficient, γ is loss coefficient, v_{gr} is group velocity of the wave in the waveguide. In principle, at a small modulation of the dielectric constant, the coupling coefficient and the loss coefficient can be found analytically [1]. However, at the modelled modulation shown in Figure 2, a fairly strong discrepancy in Q-factor arises between the results of CST modeling and the analytical theory. To improve convergence, the following approximation was used. Within the CST code, frequency dependences of the reflection factor at different lengths of the Bragg structure were modeled, and then they were compared with the analytical formula for the reflection factor at the Bragg frequency that follows from (9):

$$\begin{aligned} R(\alpha, \gamma, l) &= \\ &= \frac{i\alpha \sinh(l\sqrt{\gamma^2 + \alpha^2})}{-i\gamma \sinh(l\sqrt{\gamma^2 + \alpha^2}) + \sqrt{\gamma^2 + \alpha^2} \cosh(l\sqrt{\gamma^2 + \alpha^2})}, \end{aligned} \quad (10)$$

where l is length of the Bragg structure.

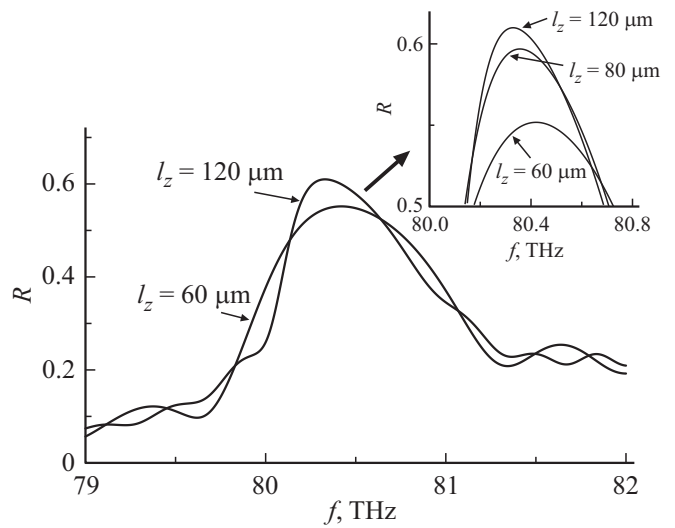


Figure 3. Frequency dependences of the mode reflection factor of a planar dielectric waveguide on the Bragg structure for various lengths.

Expression (10) allows estimating the coupling and loss coefficients from the following algebraic equations:

$$\begin{cases} R(\alpha, \gamma, l_1) = R_1 \\ R(\alpha, \gamma, l_2) = R_2 \end{cases} \quad (11)$$

The dependences of the reflection factor on frequency for various lengths of the corrugated region are shown in Figure 3. The coupling and loss coefficients obtained from the solution to (8) for different pairs of grating lengths coincide to high accuracy: $\alpha \approx 180 \text{ cm}^{-1}$, $\gamma \approx 90 \text{ cm}^{-1}$.

4. Modeling of non-stationary dynamics of DFB lasers within the quasi-optical model

To study the nonlinear dynamics of DFB laser, we use a three-dimensional model, where the active region and the Bragg structure have a finite width of l_x along the lateral coordinate x . Due to the fact that the central frequency and the main direction of wave flows propagation are determined by the gain band of the active medium and Bragg condition (4), the interaction of wave flows (5) can be considered in a quasi-optical approximation, taking into account their diffraction spreading along the coordinate x . As shown in [13–15], transverse diffraction of the radiation along the coordinate x provides a condition for suppressing the excitation of the high-frequency mode of the Bragg resonator with a frequency above the Bragg oscillation band. With this approach, the coupling of partial waves on the Bragg structure and its excitation by the active layer can be described by the following system of self-consistent equations, which are derived from the Maxwell-

Bloch equations [14–16]:

$$\begin{aligned} \left(i \frac{\partial^2}{\partial X^2} \pm \frac{\partial}{\partial Z} + \frac{\partial}{\partial \tau} \right) \hat{C}_{\pm} + \hat{\gamma} \hat{C}_{\pm} + i \hat{C}_{\mp} &= \hat{P}_{\pm}, \\ \frac{\partial \hat{P}_{\pm}}{\partial \tau} + \frac{\hat{P}_{\pm}}{\hat{T}_2} &= \frac{\beta}{\hat{T}_2} \hat{C}_{\pm} \hat{\rho}, \\ \frac{\partial \hat{\rho}}{\partial \tau} + \frac{(\hat{\rho} - 1)}{\hat{T}_1} &= -\text{Re}(\hat{C}_+ \hat{P}_+^* + \hat{C}_- \hat{P}_-^*), \end{aligned} \quad (12)$$

where $X = \sqrt{\alpha \hbar x}$, $Z = \alpha z$, $\tau = \alpha v_{gr} t$ are normalized spatial coordinates and time, $\hat{\gamma} = \gamma/\alpha$ is normalized radiation loss coefficient, which describes the radiation output at an angle to the surface of the structure, $\hat{\rho} = \frac{\rho}{\rho_e}$, ρ is surface inversion density of the active medium, ρ_e is equilibrium level of inversion without laser radiation, which characterizes the pumping intensity,

$$\begin{aligned} \hat{C}_{\pm} &= C_{\pm} (b_{TE} \omega_0 / \pi \rho_e \hbar c v_{gr})^{1/2}, \\ \beta &= \pi \rho_e |\mu|^2 T_2 c a (y - y_{\text{active}}) / \alpha \hbar \omega_0 b^{TE} \end{aligned}$$

is normalized mode gain of the active medium, $\hat{T}_{1,2} = \alpha v_{gr} T_{1,2}$ are normalized relaxation times of inversion and polarization of the active medium, b^{TE} is effective waveguide thickness for the corresponding waveguide mode, μ is dipole moment,

$$\omega_0 = 2\pi c / \lambda, \quad \hat{P}_{\pm} = P_{\pm} (\pi \omega_0 / \rho_e \alpha \hbar c v_{gr} b^{TE})^{1/2},$$

P_{\pm} is surface density of resonant polarization components of the active medium:

$$P = \delta(y - y_{\text{active}}) \text{Re}(i(P_+ e^{ihz} + P_- e^{-ihz}) e^{i\omega_0 t}), \quad (13)$$

where y_{active} is position of the active layer.

Equations (12) are further studied in the balance approximation under the assumption that the polarization relaxation time T_2 is small in comparison with other time scales. Then the polarization part (12) can be reduced to the following algebraic form:

$$\hat{P}_{\pm} = \beta \hat{C}_{\pm} \hat{\rho} \quad (14)$$

and equations (12) can be reduced to the following form:

$$\begin{aligned} \left(i \frac{\partial^2}{\partial X^2} \pm \frac{\partial}{\partial Z} + \frac{\partial}{\partial \tau} \right) \hat{C}_{\pm} + \hat{\gamma} \hat{C}_{\pm} + i \hat{C}_{\mp} &= \beta \hat{C}_{\pm} \hat{\rho}, \\ \frac{\partial \hat{\rho}}{\partial \tau} + \frac{\hat{\rho} - 1}{\hat{T}_1} &= -\beta \hat{\rho} (|\hat{C}_+|^2 + |\hat{C}_-|^2). \end{aligned} \quad (15)$$

Normalized power flows of the generated radiation in the transverse direction and longitudinal direction are characterized by the following expressions:

$$\begin{aligned} W_x &= \hat{\gamma} \int_0^{L_z} \int_{-L_x/2}^{L_x/2} (|\hat{C}_+|^2 + |\hat{C}_-|^2) dX dZ, \\ W_z &= \int_{-L_x/2}^{L_x/2} (|\hat{C}_+(Z=L_z)|^2 + |\hat{C}_-(Z=0)|^2) dX. \end{aligned} \quad (16)$$

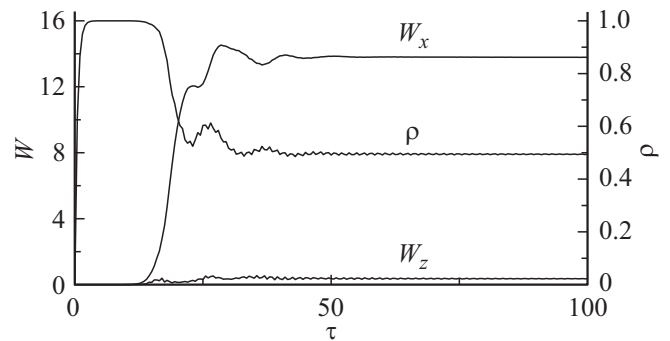


Figure 4. Time dependences of power emitted in the transverse and longitudinal directions, as well as population inversion in the center of the active region; $L_z = 10$, $L_x = 8$, $\gamma = 0.5$, $\beta = 0.8$.

It should be noted that partial waves (5) form a standing wave in the interaction region. This standing wave forms a spatial modulation of the population inversion, which is also known as the spatial hole burning effect and can be described by introducing additional spatial components of the inversion [14,15]. However, it is assumed that for the semiconductor active media under consideration this effect is suppressed by the carrier diffusion.

Initial conditions for the excitation process of a DFB laser can be represented as:

$$\begin{aligned} \hat{C}_{\pm}|_{\tau=0} &= C_0(X, Z), \\ \hat{\rho}_0|_{\tau=0} &= 0, \end{aligned} \quad (17)$$

where $C_0(x, z)$ is initial random distribution of the small-amplitude field. Boundary conditions for partial waves correspond to the absence of reflections and external energy flows along the edges of the modeling area [14,15].

The modeling results for equations (15) with the Bragg grating discussed above demonstrate a wide range of parameters for which the laser will operate in a single-frequency, single-mode operation mode. In this case, the radiation is almost completely output in the transverse direction: $W_x \gg W_z$ with negligible radiation fluxes outside the grating region towards the edges. It should be noted that, in contrast to Bragg resonators with a fixed field structure along the x axis, single-mode operation modes, taking into account the transverse diffraction losses described by equations (15), are realized in the absence of a phase jump of the grating. The process of excitation and establishment of a stationary generation mode is shown in Figure 4.

Spatial distributions of partial waves and population inversion in the stationary mode are presented in Figure 5. It can be seen that distributed losses ensure efficient use of inversion throughout the entire active volume. It is important to emphasize that the establishment of a single-mode generation takes place at the following Fresnel parameters $F = \sqrt{2\pi l_z} / l_x \sqrt{\hbar} = \sqrt{2\pi L_z} / L_x \approx 1$. Here $L_z = \alpha l_z$, $L_x \sqrt{\alpha \hbar} l_x$ are normalized values of the length and width of the interaction region. Under such conditions, the diffraction losses of the high-frequency mode in the transverse lateral

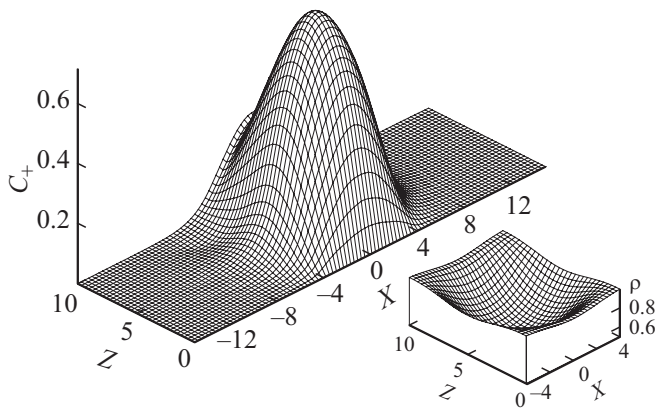


Figure 5. Spatial distribution of the field amplitude of the partial wave C_+ and the average inversion in the stationary generation mode; $L_z = 10$, $L_x = 8$, $\gamma = 0.5$, $\beta = 0.8$.

direction significantly exceed the losses of the low-frequency mode and generation is established at the frequency of the above-mentioned mode with one field variation along the above-specified coordinate.

Equations (15) also make it possible to estimate physical parameters of the linear stage of the generation process. The normalized values used in the modeling correspond to the active region length and width of $l_z \approx 1000$ μm , $l_x \approx 80$ μm and the mode gain of $\alpha\beta \approx 140$ cm^{-1} . Estimating the parameters of the stationary generation mode and, in particular, the total radiation power will require estimating the inversion energy density of the medium ρ_e and, accordingly, refining the specific laser pumping scheme and parameters.

5. Conclusion

The possibility is demonstrated of implementing a hetero-laser based on the CMT structure with the output of most of the generated radiation from the surface of the waveguide into two coherent beams using the same Bragg grating, which provides a distributed feedback. Within the CST modeling, the optimal parameters of the Bragg structure were found ensuring that up to 70% of the power to be emitted upward, while the rest of the radiation propagates into the substrate and, presumably, is scattered there.

The modeling of the lasing process within the quasi-optical approximation for electromagnetic radiation and balance equations for the active medium showed the possibility of establishing a single-frequency, single-mode lasing. Selection of modes by the transverse (lateral) index is achieved due to the difference in diffraction losses of the working and parasitic modes. In this case, the distributed radiation output at an angle to the surface ensures a fairly uniform distribution of inversion removal throughout the entire active region.

Funding

The study has been supported under the state assignment of ISP RAS on the topic No. 0030-2022-0001).

Conflict of interest

The authors declare that they have no conflict of interest.

References

- [1] H. Kogelnik. *Theory of dielectric waveguides*. In: Integrated Optics (Springer Berlin–Heidelberg, 1979) v. 7.
- [2] A. Yariv. *Quantum Electronics* (N.Y., Wiley, 1975).
- [3] G.A. Evans, J.M. Hammer. *Surface emitting semiconductor lasers and arrays* (San Diego, Academic Press, 1993).
- [4] J. Lopez, G. Witjaksono, D. Botez. *Appl. Phys. Lett.*, **75** (7), 885 (1999).
- [5] S. Li, G. Witjaksono, S. Macomber, D. Botez. *IEEE J. Select. Top. Quant. Electron.*, **9** (5), 1153 (2003).
- [6] P. Zhou, L. Niu, A. Hayat, C. Fengzhao, Z. Tianrui, Z. Xinping. *Polymers*, **11** (2), 258 (2019).
- [7] L. Can, P. Zhang, M. Xiang, X. Ma, C. Jiang, B. Tang, Q. Lu, W. Guo. *Opt. Express*, **45** (13), 3573 (2020).
- [8] K. Tian, Y. Zou, M. Guan, L. Shi, H. Zhang, Y. Xu, J. Fan, H. Tang, X. Ma. *Opt. Express*, **30**, 14243 (2022).
- [9] K.E. Kudryavtsev, V.V. Rummyantsev, V.Ya. Aleshkin, A.A. Dubinov, V.V. Utochkin, M.A. Fadeev, N.N. Mikhailov, G. Alymov, D. Svintsov, V.I. Gavrilenko, S.V. Morozov. *Appl. Phys. Lett.*, **117**, 083103 (2020).
- [10] S.V. Morozov, V.V. Rummyantsev, M.A. Fadeev, M.S. Zholudev, K.E. Kudryavtsev, A.V. Antonov, A.M. Kadykov, A.A. Dubinov, N.N. Mikhailov, S.A. Dvoretzky, V.I. Gavrilenko. *Appl. Phys. Lett.*, **111**, 192101 (2017).
- [11] A.A. Dubinov, V.V. Rummyantsev, M.A. Fadeev, V.V. Utochkin, S.V. Morozov, *FTP*, **55** (5), 455 (2021). (in Russian).
- [12] R. Kazarinov, C. Henry. *IEEE J. Quant. Electron.*, **21** (2), 144 (1985).
- [13] N.S. Ginzburg, A.S. Sergeev, E.R. Kocharovskaya, A.M. Malkin, E.D. Egorova, V.Yu. Zaslavsky. *Phys. Lett. A*, **384**, 126219 (2020).
- [14] N.S. Ginzburg, A.S. Sergeev, E.R. Kocharovskaya, A.M. Malkin, E.D. Egorova, V.Yu. Zaslavskiy, *FTP*, **54**, 974 (2020). (in Russian).
- [15] N.S. Ginzburg, A.S. Sergeev, E.R. Kocharovskaya, A.M. Malkin, V.Yu. Zaslavskiy, *FTP*, **55**, 659 (2021). (in Russian).
- [16] T.S. Mansuripur, C. Vernet, P. Chevalier, G. Aoust, B. Schwarz, Feng Xie, C. Caneau, K. Lascola, Chung-en Zah, D.P. Caffey, T. Day, L.J. Missaggia, M.K. Connors, Ch.A. Wang, A. Belyanin, F. Capasso. *Phys. Rev. A*, **94**, 063807 (2016).

Translated by Y.Alekseev